# SIMULATING NON-DARCY FLOW THROUGH POROUS MEDIA USING SUNDANCE

J. P. REESE[1], K. R. LONG[2], C. T. KELLEY[1], W. G. GRAY[3], C. T. MILLER[3]

[1]Department of Mathematics and Center for Research in Scientific Computation
North Carolina State University, Box 8205, Raleigh, NC, 27695-8205, USA
[2]Computational Science and Mathematics Research Department, Sandia National Laboratories, Livermore, CA, 94550, USA
[3]Department of Environmental Sciences and Engineering
The University of North Carolina, Chapel Hill, NC 27599-7431, USA

## Abstract

A non-Darcy partial differential equation (PDE) model for flow through porous media is presented. The focus is on the numerical implementation of the model using Sandia National Laboratories PDE simulation framework, Sundance. In particular, the discussion will include the finite element discretization and how parallelism is accomplished.

## 1. INTRODUCTION

Historically, single-phase, single-species flow through porous media has been modeled using either the linear Darcy's law or some empirical nonlinear relationship between the pressure gradient and the Darcy velocity as an *approximation* to momentum conservation. While this approach has the advantage of simplifying the flow model, there is no basis in first principles to support the use of these approximations. This lack of formalism is in stark contrast to a recent approach using microscale conservation laws and averaging techniques to methodically *derive* a macroscale momentum equation appropriate for more complex flow scenarios [GM04, GM03, GM05a, GM05b, GTS02]. Gray and Miller begin with microscale conservation laws for mass, momentum, energy, and an entropy inequality that are known to hold for all physical systems; average the equations up to the macroscale; and incorporate laws of thermodynamics to generate closure relations. The result of their Thermodynamically Constrained Averaging Theory (TCAT) approach is a closed, nonlinear, macroscale flow model based upon first principles which incorporates both a momentum conservation equation and a continuity equation.

There are two nonlinearities in the model equation guaranteeing momentum conservation. One, the inertial term, can be attributed to Forchheimer's [For01] expression for the nonlinear relationship between the pressure gradient and the Darcy velocity, $\mathbf{q}$. The other term, the advective acceleration, has the form

$$\nabla \cdot \left( \frac{\rho \mathbf{q} \ \mathbf{q}^T}{\phi} \right), \tag{1}$$

where $\mathbf{q}$ is a column vector, $\rho$ represents the fluid density, and $\phi$ denotes the porosity of the porous medium. In the literature, this term is either missing entirely from the flow

model or assumed to be negligible. The justification for this assumption is that porous media flow is always so slow that the term is insignificant in comparison to the other terms in the equation [Bea72, page 104].

However, in this paper we include the advective acceleration term in the flow model (see § 2) to more thoroughly examine its numerical contribution as the velocities of the system increase. In particular, we seek a more formal description of the significance of the nonlinearity in real systems of interest. By "real systems of interest", we refer to heterogeneous porous media. Historically this aspect of non-Darcy flow has been given little attention; in fact, the recent publications by Fourar et al. comprise much of the relevant literature [FLKFH05, PF06].

Section 3 describes the software used to simulate the porous medium flow model, the two-dimensional test problem is discussed in § 4, numerical results are provided in § 5, and § 6 contains concluding remarks.

## 2. MODEL EQUATIONS DESCRIBING SINGLE-PHASE FLOW THROUGH POROUS MEDIA

The steady-state model we consider for single-phase, single species groundwater flow through a porous medium is

$$\rho = \rho_0 \exp\left(\beta\left(p - p_0\right)\right) \tag{2}$$

$$\nabla \cdot (\rho \mathbf{q}) = \mathcal{S}' \tag{3}$$

$$\nabla \cdot \left(\frac{\rho \mathbf{q}\mathbf{q}^T}{\phi}\right) + \phi\left(\nabla p - \rho \mathbf{g}\right) + \phi R \mathbf{q} = 0, \tag{4}$$

where the unknown quantities are pressure, $p$, and Darcy velocity, $\mathbf{q}$. Additionally, $t$ represents time, $\mathbf{g}$ represents gravitational acceleration, and external mass sources/sinks are represented in the continuity equation (3) by $\mathcal{S}'$.

The stress tensor, $R$, in the momentum equation is based upon Forchheimer's nonlinear relationship between the Darcy velocity and the pressure gradient. Specifically,

$$R = \frac{A\left(1-\phi\right)^2 \mu}{D^2 \phi^4} + \frac{B\rho\left(1-\phi\right)|\mathbf{q}|}{D\phi^5}, \tag{5}$$

where $A$ is the inverse of dimensionless hydraulic conductivity [Mil05], $B$ is an experimentally derived constant [PHM01], $D$ is the surface average grain diameter of the porous medium, and $\mu$ is the dynamic viscosity of the fluid.

## 3. SOFTWARE

To solve the system of PDEs in (3) and (4), we use the Sundance object-oriented PDE simulation framework from Sandia National Laboratories. Its underlying solver capabilities are contained in another Sandia software framework, Trilinos, and a description of the two frameworks follows.

3.1. **Sundance.** Sundance [Lon04] is a system for specifying, building, and applying parallel finite element approximations to general PDEs. Sundance consists of user-callable components written in C++ (with optional Python wrappers) that allow the user to

specify the PDE and associated boundary conditions in weak form using operator overloading on a family of symbolic objects. The Sundance symbolic objects and operators can be used to assemble virtually any PDE. Each test or unknown function in a Sundance problem is constructed with a specifier of its finite-element basis, and any integral can be given a specifier for the type and order of quadrature rule to be used. Stabilization terms can be added at the symbolic level; typically, these involve the mesh size $h$, so a special symbolic object `CellDiameterExpr` has been created which when evaluated, refers to the mesh to obtain a numerical value of $h$ on each element. The ability to specify basis, quadrature, and optional stabilization terms gives the Sundance user fine control over the discretization process.

Since it is easy to change the equation and/or the boundary conditions, it is easy to experiment with different models by making a small number of changes to Sundance-based simulation code. The symbolic problem setup capability of Sundance is useful not only for rapid development of forward simulators such as our flow model, but even more importantly, it makes possible the concurrent specification of gradient and/or adjoint equations, greatly facilitating the application of gradient-based optimization methods. Because a Sundance simulator has a symbolic representation of the problem at hand, gradients can be evaluated using automatic, in-place differentiation concurrently with evaluation of objective functions and residuals.

3.2. **Trilinos.** Sundance does the work of assembling matrices and vectors in parallel from a problem specification; computations on those mathematical objects are then done using the Trilinos family of solver components [HBH+05]. Trilinos includes a high-performance, low-level matrix/vector library (EPetra), incomplete factorization preconditioners (IFPACK), algebraic multilevel solvers and preconditioners (ML), Krylov solvers (Belos), and nonlinear solvers (NOX). Trilinos also provides a set of abstract interfaces, Thyra, allowing interoperability with other solver libraries.

Both Sundance and Trilinos are freely available under the lesser Gnu Public License.

## 4. TEST PROBLEM DESCRIPTION

We simulate two-dimensional steady-state groundwater flow through a heterogeneous porous medium using the TCAT model ((3) and (4)). The goal is to determine the significance of the nonlinear terms in the flow model; in particular, we focus on the advective acceleration term shown in (1).

We will compare the numerical contribution of (1) to that of the linear portion of equation (5) as the steady-state velocity of the system increases. We fix the pressure gradient across the domain to induce flow, while the other two boundaries exhibit no flow conditions. In this case, we have no external sources/sinks of mass, so $\mathcal{S}' = 0$.

The domain of interest, $\Omega$, is shown in Figure 1 as a square of dimension $[0, 1\text{ km}] \times [0, 1\text{ km}]$. The top, right, bottom, and left boundaries of the domain are denoted $\Gamma_T, \Gamma_R, \Gamma_B$, and $\Gamma_L$ respectively. The fixed pressure boundaries are $\Gamma_L$ and $\Gamma_R$, while the no flow boundary condition on $\Gamma_T$ and $\Gamma_B$ implies that $\mathbf{q} \cdot \mathbf{n} = 0$ there where $\mathbf{n}$ is the unit outward normal vector to the boundary.

4.1. **Weak formulation.** To use Sundance to solve the system of equations (3) and (4) with the finite element method, we first write the system of equations in weak form. While

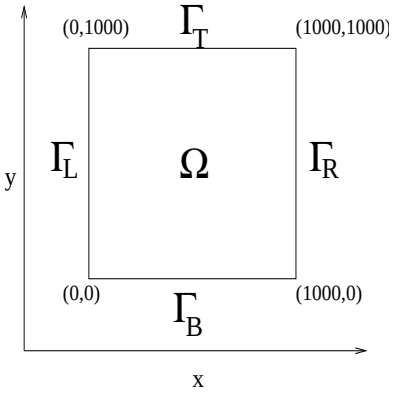


FIGURE 1. Test problem domain

Sundance allows the unknowns to be represented by different basis functions, due to memory constraints imposed by our computing architecture we must represent the pressure and velocity unknowns using the same basis functions. To stabilize this discretization, we incorporate pressure stabilization techniques by adding a term of the form $\beta h^2 \nabla^2 p$ to the mass equation where $h$ is the diameter of the finite element cell (see § 3.1). This choice is a simplified version of the stabilization techniques of Hughes [FH93, HH92].

We use the notation $\hat{p}$ and $\hat{\mathbf{q}}$ for the pressure and velocity test functions, respectively. Prior to specifying the weak form of the PDE within Sundance, we define $p, \hat{p}, \mathbf{q}$, and $\hat{\mathbf{q}}$ to be Lagrange interpolation polynomials of degree one. The system of equations (6) and (7) provides the resulting weak form of our test problem. Note that in equation (7), the expansion for $R$ is considered to be equation (5) with the density equation of state from equation (2) substituted in the quadratic term.

$$\int_\Omega \beta h^2 \nabla p \cdot \nabla \hat{p} \, \mathrm{d}\Omega - \int_\Omega \rho_0 \exp\left(\beta \left(p - p_0\right)\right) \mathbf{q} \cdot \nabla \hat{p} \, \mathrm{d}\Omega = 0 \tag{6}$$

$$\int_\Omega \nabla \cdot \left( \frac{\rho_0 \exp\left(\beta \left(p - p_0\right)\right) \mathbf{q}\mathbf{q}^T}{\phi} \right) \cdot \hat{\mathbf{q}} \, \mathrm{d}\Omega + \int_\Omega \phi \nabla p \cdot \hat{\mathbf{q}} \, \mathrm{d}\Omega = -\int_\Omega \phi R \mathbf{q} \cdot \hat{\mathbf{q}} \, \mathrm{d}\Omega \tag{7}$$

As for boundary conditions, the no flow boundary conditions on $\Gamma_T$ and $\Gamma_B$ are implicit in the weak form, but the Dirichlet pressure boundary conditions must still be specified on $\Gamma_L$ and $\Gamma_R$. Thus, (6) and (7) together with

$$p = p_L \text{ on } \Gamma_L \tag{8}$$

$$p = p_R \text{ on } \Gamma_R \tag{9}$$

define the weak form of the test problem where the constants $p_L$ and $p_R$ denote the fixed pressure value on $\Gamma_L$ and $\Gamma_R$, respectively.

4.2. **HETEROGENEITY.** In addition to the weak form of the model equations we need a representation for the heterogeneous medium which is input for the flow model via the parameter $A$ in equation (5). We assume that the hydraulic conductivity of most natural porous medium systems is log-normally distributed [DS98, page 38], and

determine the spatial correlation between hydraulic conductivity values across the domain using a Gaussian variogram, shown in equation (10).

Several algorithms exist to generate a random field exhibiting a standard normal distribution with spatial correlation; turning bands, sequential Gaussian algorithm, and the fast Fourier transform (FFT) are a few examples [DJ98, pages 120-122, 139-148]. The simulations shown here use s sequential Gaussian algorithm as explained in [DJ98, section V.2.3]; a specific implementation of this algorithm, `sgsim`, is distributed within the Geostatistical Software LIBrary (GSLIB). GSLIB source code, documentation, and executables can be found at the website `http://www.gslib.com/`, and further documentation is provided in the text [DJ98].

Table 1 provides an explanation of the input parameters required for `sgsim`. The goal is to generate a log-normally distributed and spatially correlated random field of $100 \times 100$ homogeneous blocks to approximate a realistic hydraulic conductivity field over a square domain of dimension $[0, 1 \text{ km}] \times [0, 1 \text{ km}]$. We choose a correlation length of 100 meters and 102 nodes per dimension over the area $[-5, 1005] \times [-5, 1005]$. Thus, there are approximately ten correlation lengths in each dimension and ten nodes per correlation length. A Gaussian model given by

$$\gamma(d) = c\left[1 - exp\left(-\frac{9d^2}{a^2}\right)\right] \tag{10}$$

was used to determine the correlation between two locations separated by a distance $d$. This model is defined by the sill, $c$, and correlation length $a$.

| Parameter | Definition | Value |
|---|---|---|
| `nx` | number of nodes in $x$ direction, similarly for $y$ | 102 |
| `xmn` | location of first $x$ node (origin of $x$ axis), similarly for $y$ | -5.0 |
| `xsiz` | spacing of nodes in $x$ direction, similarly for $y$ | 10.0 |
| `seed` | integer seed to the pseudorandom number generator | 69069 |
| `nst` | number of nested variogram structures | 1 |
| `c0` | isotropic nugget effect | 0 |
| `it` | integer flag specifying type of variogram model | 3 |
| `cc` | sill (note: `c0`+`cc`=1.0) | 1.0 |
| `ang1` | angle defining orientation of an ellipsoid in 3D | 0.0 |
| `ang2` | angle defining orientation of an ellipsoid in 3D | 0.0 |
| `ang3` | angle defining orientation of an ellipsoid in 3D | 0.0 |
| $\texttt{aa}_{hmax}$ | correlation range in horizontal maximum direction | 100.0 |
| $\texttt{aa}_{hmin}$ | correlation range in horizontal minimum direction | 100.0 |
| $\texttt{aa}_{vert}$ | correlation range in vertical direction | 100.0 |

TABLE 1. GSLIB PARAMETERS. Input parameters for `sgsim` to generate a field variable with mean zero and standard deviation one [DJ98, pages 170-174,330-336].

## 5. NUMERICAL RESULTS

Table 2 provides most of the model parameter values used to perform the Sundance simulations in this section. However, numerical values for the grid-dependent parameters $\beta$ and $h$ appear in Table 3. The Trilinos nonlinear solver, NOX, was used to solve the nonlinear system associated with the TCAT flow model by Newton's method with a linesearch globalization. To compute the Newton step, we used the BICGSTAB Krylov method preconditioned with domain decomposition and incomplete LU factorizations on the subdomains. In particular, the Trilinos packages TSF and IFPACK define the linear solver and preconditioner, respectively. Furthermore, preconditioning in this fashion is the default when using TSF linear solvers.

The heterogeneous field generated using GSLIB is defined at the nodes of a $100 \times 100$ grid, but one can see that the grid refinement in Table 3 begins with a $400 \times 400$ grid. This is because the 400 grid is the first grid on which the field structure (i. e. block heterogeneity) becomes apparent due to the existence of multiple nodes in the interior of each grid cell. The grid refinement study was performed by comparing only pressure

| Parameter | Value | Equation(s) |
|---|---|---|
| $\beta$ | grid dependent stabilization parameter | (6) |
| $h\,(\mathrm{m})$ | grid dependent cell diameter parameter | (6) |
| $A$ | log-normally distributed, spatially correlated random field | (5) |
| $\rho\left(\frac{\mathrm{kg}}{\mathrm{m}^3}\right)$ | 1000.0 | (4) and (5) |
| $\phi$ | 0.442 | (4) and (5) |
| $\mathbf{g}\left(\frac{\mathrm{m}}{\mathrm{s}^2}\right)$ | $\mathbf{0}$ | (4) |
| $B$ | 2.4194 | (5) |
| $\mu\left(\frac{\mathrm{kg}}{\mathrm{m\text{-}s}}\right)$ | 0.00114 | (5) |
| $D\,(\mathrm{m})$ | 1.9996e-04 | (5) |

TABLE 2. MODEL PARAMETERS.

nodes on successively finer grids. The pressure values computed on an $N \times N$ grid are denoted by $P_N$, while the error on that same grid is given by $E_N$. We define

$$E_N \equiv \frac{\|P_N - P_{2N}^N\|_2}{N+1}, \tag{11}$$

where $P_{2N}^N$ denotes that while the pressure values were computed using the $2N \times 2N$ grid, in this error computation we are only using the values which correspond to spatial locations on the $N \times N$ grid (i.e. points common to both the $N \times N$ and $2N \times 2N$ grids).

As $N \to \infty$, the ratio $\frac{E_N}{E_{2N}}$ will approach the order of the method. Since $\frac{E_{800}}{E_{1600}} = 4.2$, we appear to have resolved the heterogeneity enough to see the second order convergence we expect from our solution strategy. However, to truly guarantee second order convergence we should solve the TCAT model on a $6400 \times 6400$ grid so that the extra data point $E_{3200}$ can be computed. Unfortunately, the increased memory requirements of the $6400 \times 6400$ grid require at least 125 processors. It is difficult to obtain that many dedicated processors on our blade cluster; thus, we leave that fine grid computation for a later date.

| Grid | $\beta$ | $h$ | Error | Avg. Krylovs/Newton |
|---|---|---|---|---|
| 400 | 4.0e-08 | 2.5 | $E_{400}$=16.8103 | 101 |
| 800 | 8.0e-07 | 1.25 | $E_{800}$=12.8317 | 322 |
| 1600 | 4.0e-05 | 0.625 | $E_{1600}$=3.0593 | 288 |
| 3200 | 4.0e-03 | 0.3125 | | 298 |

TABLE 3. GRID REFINEMENT.

To test the scalability of the simulator we compare the run time for three different grids in Table 4. Starting with the $400 \times 400$ grid run on two processors, we simultaneously quadruple the number of unknowns and the number of processors used to run the simulation. For the simulator to scale well, the run times should be approximately constant, and in Table 4 one can see that this is the case. Thus, this simulator scales well as the number of processors increases.

| Grid | # Processors | Total Time (min.) | Nonlinear Solver Time (min.) |
|---|---|---|---|
| 400 | 2 | 42.9 | 41.3 |
| 800 | 8 | 45.0 | 43.3 |
| 1600 | 32 | 48.0 | 46.2 |

TABLE 4. PARALLEL SCALABILITY.

## 6. CONCLUSIONS

We have shown that using the Sundance framework to simulate single-phase, single-species groundwater flow through a porous medium in two spatial dimensions results in second order convergence in pressure once the grid is fine enough to fully resolve the heterogeneity of the porous medium. Furthermore, the simulator is shown to have almost perfect parallel scalability. It appears that this strategy is a sufficient method to use for future examination of the advective acceleration term.

## ACKNOWLEDGMENTS

The research of CTK and JPR was supported by Army Research Office grants #DAAD19-02-1-0391, #W911NF-05-1-0171, #DAAD19-02-1-0111 and National Science Foundation grants #DMS-0404537 and #DMS-0209695. JPR was also supported by a US Department of Education GAANN fellowship. WGG and CTM are supported by National Science Foundation grant #DMS-0327896. Sandia is a multiprogram laboratory operated by Sandia Corporation, a Lockheed Martin Company, for the United States Department of Energy's National Nuclear Security Administration under contract DE-AC04-94AL85000.

We would also like to thank the North Carolina State University High-Performance Computing group for access to the IBM Blade Center. In particular, Eric Sills and Gary Howell provided hardware and software support.

## References


[Bea72] Jacob Bear. *Dynamics of Fluids in Porous Media*. Dover Publications, Inc., New York, 1972.

[DJ98] Clayton V. Deutsch and André G. Journel. *GSLIB Geostatistical Software Library and User's Guide*. Applied Geostatistics Series. Oxford University Press, New York, second edition, 1998.

[DS98] Patrick A. Domenico and Franklin W. Schwartz. *Physical and Chemical Hydrogeology*. John Wiley and Sons, Inc., New York, NY, second edition, 1998.

[FH93] L. P. Franca and T. J. R. Hughes. Convergence analysis of Galerkin least squares methods for the symmetric advective-diffusive form of the Stokes and incompresible Navier-Stokes equations. *Comp. Meth. Appl. Math. Eng.*, 2:285–298, 1993.

[FLKFH05] M. Fourar, R. Lenormand, M. Karimi-Fard, and R. Horne. Inertia effects in high-rate flow through heterogeneous porous media. *Transport in Porous Media*, 60:353–370, 2005.

[For01] P. Forchheimer. Wasserbewegun durch boden. *Z. Ver. Deutsch. Ingen.*, 45:1782–1788, 1901.

[GM03] William G. Gray and Cass T. Miller. Multiphase transport phenomena. Department of Environmental Sciences and Engineering, University of North Carolina, unpublished lecture notes for ENVR265, 2003.

[GM04] W. G. Gray and C. T. Miller. Examination of Darcy's law for flow in porous media with variable porosity. *Environmental Science & Technology*, 38(22):5895–5901, 2004.

[GM05a] William G. Gray and Cass T. Miller. Thermodynamically Constrained Averaging Theory approach for modeling flow and transport phenomena in porous medium systems: 1. Motivation and overview. *Advances in Water Resources*, 28:161–180, 2005.

[GM05b] William G. Gray and Cass T. Miller. Thermodynamically Constrained Averaging Theory approach for modeling flow and transport phenomena in porous medium systems: 2. Foundation. *Advances in Water Resources*, 28:181–202, 2005.

[GTS02] William G. Gray, Andrew F. B Tompson, and Wendy E. Soll. Closure conditions for two-fluid flow in porous media. *Transport in Porous Media*, 47(1):29–65, April 2002.

[HBH+05] M. Heroux, R. Bartlett, V. Howle, R. Hoekstra, J. Hu, T. Kolda, R. Lehoucq, K. Long, R. Pawlowski, E. Phipps, A. Salinger, H. Thornquist, R. Tuminaro, J. Willenbring, A. Williams, , and K. Stanley. An overview of the Trilinos project. *ACM Transactions on Mathematical Software*, 31(3), 2005.

[HH92] Isaac Harari and Thomas J. R. Hughes. What are $c$ and $h$? inequalities for the analysis and design of finite element methods. *Compute Methods in Applied Mechanics and Engineering*, 97:157–192, 1992.

[Lon04] Kevin Long. Sundance 2.0 tutorial. Technical Report SAND2004-4793, Sandia National Laboratories, 2004.

[Mil05] Cass T. Miller. Email communication, June 2005. Topic: motivating heterogeneous simulations and clarifying the meaning of $A$ in resistance expression ("... hydraulic conductivity for the standard model or $A^{-1}$ for your model...").

[PF06] M. Panfilov and M. Fourar. Physical splitting of nonlinear effecs in high-velocity stable flow through porous media. *Advances in Water Resources*, 29:30–41, 2006.

[PHM01] Chongxun Pan, Markus Hilpert, and Cass T. Miller. Pore-scale modeling of saturated permeabilities in random sphere packings. *Physcial Review E*, 64(6):1–9, December 2001.